



# Erosion and thermal desorption characteristics of 1D-CF/B<sub>4</sub>C composite

Takahiro Yamaki <sup>a,\*</sup>, Yasutaka Suzuki <sup>a</sup>, Akio Chiba <sup>a</sup>, Mitsuo Nakagawa <sup>a</sup>,  
Yoshitaka Gotoh <sup>a</sup>, Ryutarou Jimbou <sup>b</sup>, Masahiro Saidoh <sup>b</sup>

<sup>a</sup> Hitachi Research Laboratory, Hitachi Ltd. 1-1 Saiwai-cho, 3-chome, Hitachi-shi, Ibaraki-ken 317, Japan

<sup>b</sup> Naka Fusion Research Establishment, JAERI, 801-1 Mukouyama, Naka-machi, Naka-gun, Ibaraki-ken 311-01, Japan

## Abstract

Erosion and thermal desorption characteristics under 3 keV D<sub>3</sub><sup>+</sup> irradiation were investigated for 1D-carbon fiber (CF)/B<sub>4</sub>C composites (30 to 80 CF vol%), at surface cut normal to the CF axis. Chemical sputtering rate of 1D-CF/B<sub>4</sub>C sintered at 2100°C was lower at the CF sections than that of pure graphite, due to solid solution of boron into the CF core. On the other hand, in the case of those at below 1800°C, suppression of chemical sputtering was not observed at the center part of the CF sections. From TDS results, it is considered that the boron diffusion depths into CF do not depend on the B<sub>4</sub>C volume fraction, but on the sintering temperature.

**Keywords:** Desorption; Chemical erosion; Low Z wall material

## 1. Introduction

Boron and boron carbide-overlaid graphite are hopeful candidates for plasma facing material (PFM) of experimental nuclear fusion reactor. It is well known that boron and boron carbide have lower hydrogen retention and lower chemical sputtering yield for hydrogen and oxygen ion irradiation, compared to graphite [1–3]. However, because of their lower thermal conductivities, the thicknesses of these overlayers had to be limited to below 200 μm [4].

Recently, carbon fiber (CF) reinforced B<sub>4</sub>C composite (CF/B<sub>4</sub>C) for PFM with long life time has been developed by using hot-pressing method. The CF/B<sub>4</sub>C has thermal conductivity at around 250 W/mK (at 25°C) and endures thermal shocks to more than 23 MW/m<sup>2</sup> × 5 s electron beam heat loading [5], because of its CF's textures oriented normal to the surface interacting with the plasma surface. On the other hand, the erosion characteristics of the composite are not yet clearly understood because of the coexis-

tence of graphite and B<sub>4</sub>C phases at the plasma facing surface.

In the present study, erosion characteristics under 1 keV D<sup>+</sup> (3 keV D<sub>3</sub><sup>+</sup>) irradiation are investigated for 1D-CF/B<sub>4</sub>C composites, of CF vol% varied from 30 to 80%, within which the CF's were oriented normal to the surface. Chemical sputtering suppression of the CF phase in the 1D-CF/B<sub>4</sub>C's, due to boron diffusion, is discussed, and related to thermal desorption spectroscopy (TDS) results.

## 2. Experimental

### 2.1. Specimens

Specimens for the present study are listed in Table 1. 1D-CF/B<sub>4</sub>C, with the volume fraction of unidirectionally oriented CF (*V<sub>f</sub>*) varied in a 0–80% range, were made through a hot pressing method. A green sheet of unidirectionally stacked CF (10 μm diameter, thermal conductivity 520 W/mK, type P-120S, AMOCO) with impregnation of B<sub>4</sub>C powder (1.46 μm mean diameter, Idemitsu Material) slurry was sintered at 1700–2100°C for 1 h at 30 MPa.

\* Corresponding author. Tel.: +81-294 23 5773; fax: +81-294 23 6995.

Table 1  
Specimens

Specimen	$V_f$ (vol%)	Sintering temp. (°C)	Density (g/cm <sup>3</sup> )
ID-CF/B <sub>4</sub> C			
P30(2100)	30	2100	2.24
P50(2100)	50	2100	2.26
P65(1700)	65	1700	1.86
P65(1800)	65	1800	2.01
P65(2100)	65	2100	2.21
P80(2100)	80	2100	2.18
Hot pressed B <sub>4</sub> C	0	2100	2.40
Isotropic graphite	—	—	1.82
Felt-CFC	—	—	1.81

Specimens of 10 × 10 × 2 mm dimension were fabricated from a sintered body so as the CF axes to be oriented normal to the specimen surface. Specimen surfaces were polished with #3000 mesh diamond powder sheet.

Fig. 1 shows a SEM image of polished specimen surface of ID-CF/B<sub>4</sub>C specimen, sintered at 2100°C (P50(2100)). The specimen, being sintered to almost theoretical density, has been polished to a mirror-like surface as shown in Fig. 1. However, in the cases of specimens sintered below 1800°C, which are still low in density, the polished surfaces showed much voids, and were ground faster than the CF phase.

CF-felt-reinforced carbon composite (Felt-CFC: size 10 × 10 × 2 mm, cut normal to the felt reinforcement plane, type PCC-2S, Hitachi Chemical) and isotropic graphite (size 10 × 10 × 2 mm, type PD-330S, Hitachi Chemical) were used as reference materials. A hole (0.8 mm diameter, 3–4 mm depth) was bored into each of those

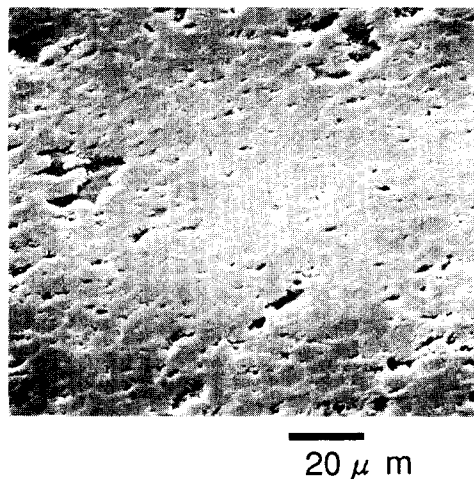


Fig. 1. SEM image of a polished surfaces of ID-CF/B<sub>4</sub>C, P50(2100), sintered at 2100°C.

specimens at a side face for insertion of a thermocouple element.

## 2.2. Experimental apparatus

Both erosion yield and TDS experiments were performed by using an ion irradiation apparatus composed of an ion source, a mass separator, and an ultra high vacuum specimen chamber (volume: 0.008 m<sup>3</sup>), details of which have been described elsewhere [6]. The chamber was equipped with a Faraday cup for ion beam current measurement, a tantalum filament for radiation or electron beam bombardment heating at the rear face of the specimen, a quadrupole mass spectrometer (QMS) for TDS, and a W-5Re/W-26Re thermocouple for specimen temperature measurement. The chamber is equipped with a turbo-molecular pump with an effective pumping speed of 0.2 m<sup>3</sup>/s.

## 2.3. Erosion yield measurement

Erosion yields were measured through the weight-loss method [1]. Prior to the erosion experiment, the specimens were degassed at 1350 K (in the case of B<sub>4</sub>C:1000 K) for a few minutes at below 8 × 10<sup>-4</sup> Pa. Then a 3 keV D<sub>3</sub><sup>+</sup> beam of a 7.5 mm diameter, irradiated at the specimen at normal incidence at 550–1100 K, at a flux of (5–6) × 10<sup>15</sup> D/cm<sup>2</sup>s to a total amount of (8.5–11) × 10<sup>19</sup> D atoms. Before and after the D<sub>3</sub><sup>+</sup> irradiation experiment, the weight measurements were made with a micro-balance in air atmosphere.

The erosion yield,  $Y$ , was determined from the following equation:

$$Y = -\Delta W(N_A/A)/(\Phi S), \quad (1)$$

where  $\Delta W$  is the weight gain of the specimen due to the net erosion, i.e. after correction for the weight changes due to evaporation and sublimation of the specimen and due to deposition of the heater material, which was determined from heating experiments without ion irradiation.  $A$  is the mean atomic weight of the ID-CF/B<sub>4</sub>C determined from the following equation:

$$A = (12.00V_f + 11.04(1 - V_f))/100. \quad (2)$$

$N_A$  is Avogadro's constant,  $\Phi$  is the ion fluence, and  $S$  is the irradiation area.

After the erosion experiment, SEM observations of the irradiated surfaces were made.

## 2.4. TDS analysis

Specimens were irradiated in situ with 3 keV D<sub>3</sub><sup>+</sup> ion beam of a 6.5 mm diameter to 2 × 10<sup>18</sup> D/cm<sup>2</sup> at 400–1000 K. After the specimen temperature reached below 400 K, D<sub>2</sub> ( $M/e = 4$ ) and CD<sub>4</sub> ( $M/e = 20$ ) QMS signal intensities were recorded as the specimen temperature was

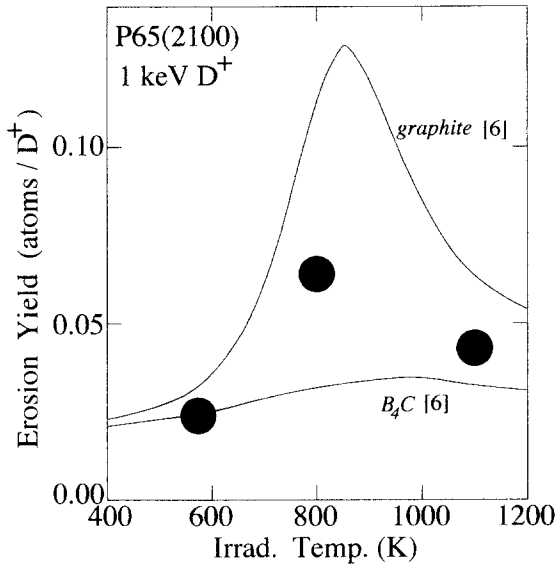


Fig. 2. Temperature dependence of the erosion yield of 1D-CF/B<sub>4</sub>C, P65(2100).

raised from 400 to 1400 K (in the case of B<sub>4</sub>C: to 1300 K) at a constant ramp rate of 1 K/s. The specimen was degassed in situ at 1473 K for a few minutes after each TDS experiment, a series of measurements at different irradiation temperatures were performed sequentially.

3. Experimental results

3.1. Erosion yield measurement results

Fig. 2 shows erosion yields of P65(2100) in a 550–1100 K range, compared to graphite and B<sub>4</sub>C data reported by

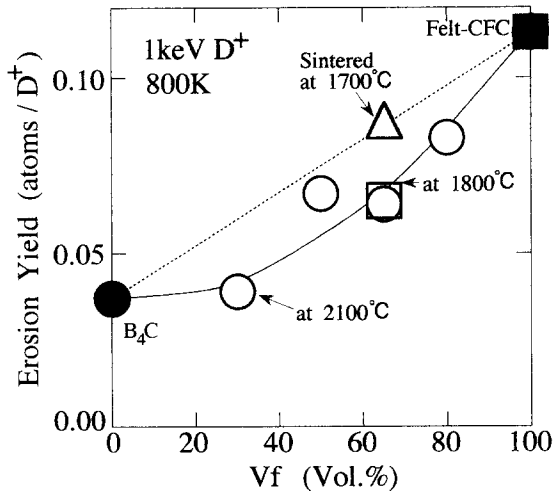


Fig. 3.  $V_f$  dependence of the erosion yield of B<sub>4</sub>C, 1D-CF/B<sub>4</sub>C and CFC irradiated at 800 K.

Roth [7]. As shown in this figure, the erosion yield of P65(2100) are in between graphite and B<sub>4</sub>C data.

Fig. 3 shows erosion yield data for B<sub>4</sub>C, 1D-CF/B<sub>4</sub>C ( $V_f$ : 30–80 vol%) sintered at 2100°C, 1800°C, and Felt-CFC as a function of  $V_f$  (i.e., graphite vol%) irradiated at 800 K. The dotted line shows calculated results of

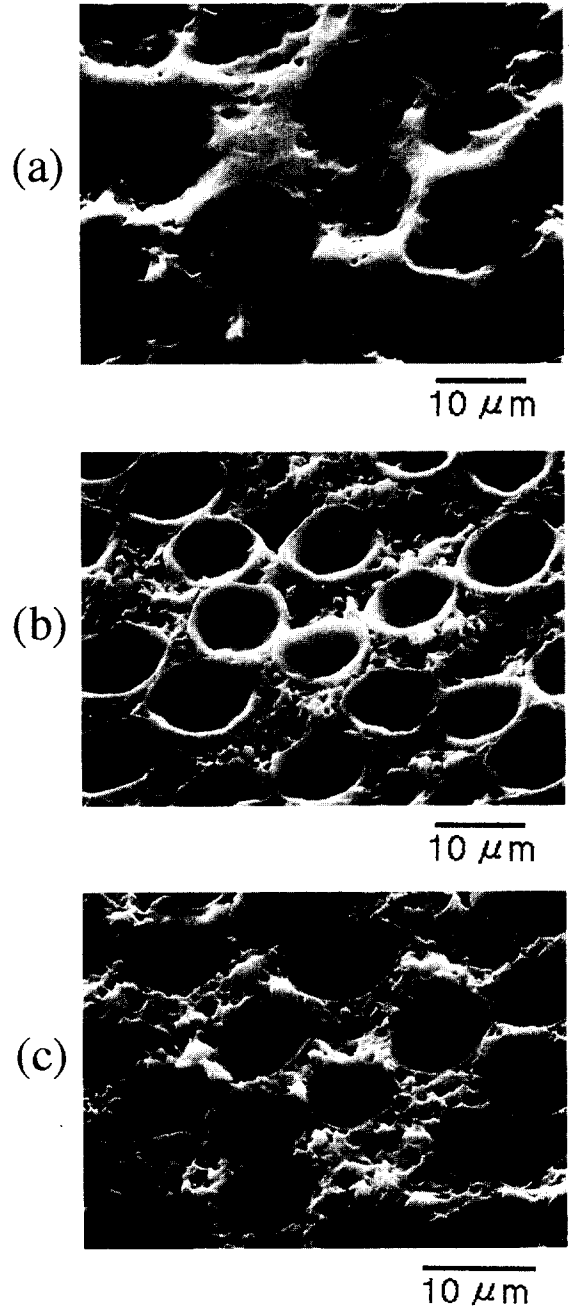


Fig. 4. SEM images of D<sup>+</sup> irradiated surfaces of (a) P50(2100), (b) P66(1800) and (c) P65(1700) specimen after the erosion experiment at 800 K.

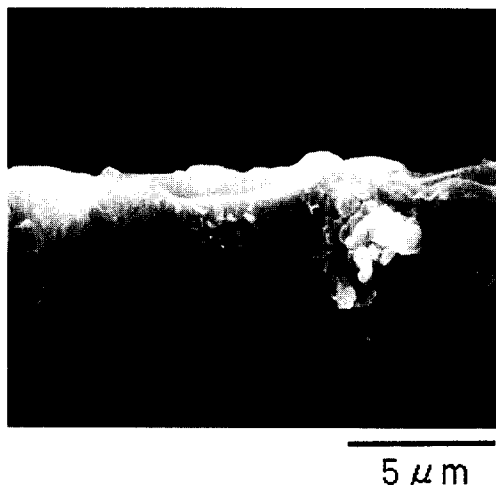


Fig. 5. SEM image of a vertical section of the sub-surface layer of P65(1800) specimen after erosion experiment at 800 K.

erosion yield from the following equation assuming a simple sum rule:

$$Y_c = \{Y_{CFC}V_f + Y_{B_4C}(1 - V_f)\} / 100, \quad (3)$$

where  $Y_{CFC}$  and  $Y_{B_4C}$  are the erosion yields for Felt-CFC of pure graphite phase and  $B_4C$ , respectively.

As shown in this figure, the erosion yields of 1D-CF/ $B_4C$  sintered at above 1800°C were found to be lower than those calculated values (dotted line), indicating that the chemical sputtering rates of these CF in 1D-CF/ $B_4C$  are lower than for pure graphite.

### 3.2. SEM analysis

Fig. 4a–c shows SEM images of the  $D^+$  irradiated surfaces of P50(2100), P65(1800) and P65(1700) specimens after the erosion experiments at 800 K. In the case of P50(2100), the eroded surfaces of the CF section were almost ‘flat’, while, in the case of both P65(1800) and P65(1700), they were ‘hollow’, indicating that the sputtering rate of the CF is higher at the center part than that at the periphery. Fig. 5 shows a SEM image of a vertical section of the P65(1800) specimen after the erosion experiment, which clearly shows that sputtering rate difference between at the center and at the outer part.

### 3.3. TDS analysis

Fig. 6 shows  $D_2$ - and  $CD_4$ -TDS of  $B_4C$ , 1D-CF/ $B_4C$  (P30(2100) and P80(2100)) and graphite after 1 keV  $D^+$  irradiation. The  $D_2$ -TDS of graphite shows a maximum at around 900–1100 K, which is also observed for pure graphite or carbon phase [8]. For  $B_4C$ , a  $D_2$  peak was observed at around 600 K and 800 K. As for 1D-CF/ $B_4C$ , the main  $D_2$  peak was observed at around 850 K.

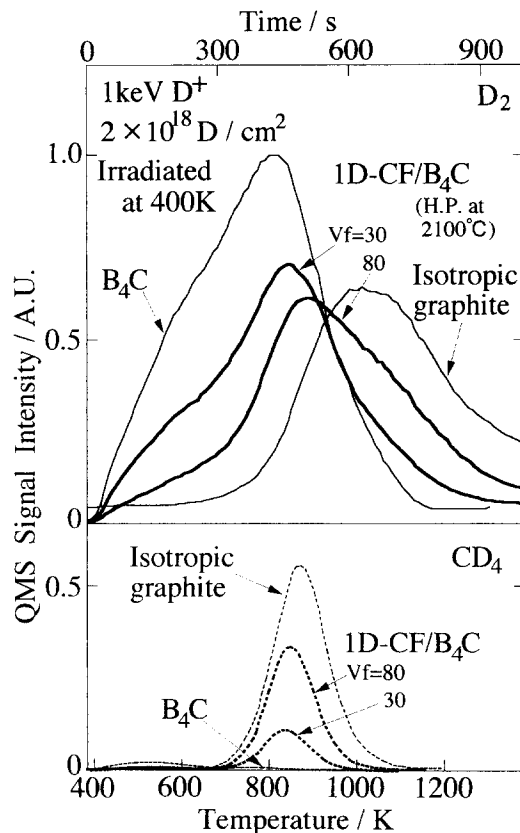


Fig. 6.  $D_2$ - and  $CD_4$ -TDS spectra of  $B_4C$ , P30(2100), P80(2100) and graphite after 1 keV  $D^+$  irradiation at 400 K.

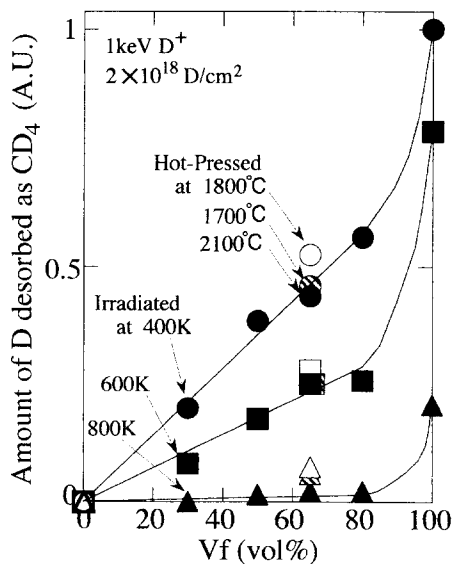


Fig. 7.  $V_f$  dependence of the relative amount of desorbed  $CD_4$  after  $D^+$  irradiation of  $2 \times 10^{18} D/cm^2$  at different temperature.

The  $CD_4$ -TDS of graphite shows a peak at around 850 K, and for  $B_4C$ , the  $CD_4$  peak was observed at around 550 K and 750 K, but the amount of desorbed  $CD_4$  was almost negligible compared to that for pure graphite. As for 1D-CF/ $B_4C$ , the  $CD_4$  peak was observed at by 10–20 K lower temperatures than those of graphite.

Fig. 7 shows the  $V_f$  dependence of the relative amount of D desorbed as  $CD_4$  from the specimens (the amount of that for graphite irradiated at 400 K was defined as 1.0) after irradiation of  $D^+$  at 400–800 K. In the case of 1000 K irradiation, the amount of desorbed  $CD_4$  was at an almost negligible level for all of the specimens.

The amount of desorbed  $CD_4$  from P65(1700) and P65(1800) was higher than that from P65(2100). Furthermore, from Fig. 7 it is clear that the amount of desorbed  $CD_4$  from 1D-CF/ $B_4C$  sintered at 2100°C is proportional to the  $V_f$ , i.e. the surface area density of the CF's in 0 to 80% range.

#### 4. Discussion

For chemical sputtering processes in graphite, first, 'precursor for  $CD_4$ ' are considered to be generated within the ion implantation layer under  $D^+$  irradiation, which react with trapped deuterium to be finally desorbed as  $CD_4$  depending on the irradiation temperature, the ion flux and the ion range. The  $CD_4$ -TDS signal indicates that both  $CD_4$  and/or  $CD_4$  precursors remain in the irradiated sample [8]. It is well known that a solid solution of a few percent boron suppresses chemical sputtering of graphite [9–11], but only at above 600 K [12], which may be explained through the fact that the solid solution of boron in graphite effects decreasing of the activation energy for  $D_2$  formation and desorption, which then lead to a decrease in the D concentration necessary for  $CD_4$  formation [8].

Previous TDS experiments on boron/carbon sputter films after 1 keV  $D^+$  irradiation have shown that a main  $D_2$  peak is observed at around 850 K, at by 200 K lower temperature, and a  $CD_4$  peak at a slightly lower temperature than those of carbon sputter film. It has been concluded that the 850 K peak is due to graphite phase with boron solution. As shown in Fig. 6, for the 1D-CF/ $B_4C$ , the main  $D_2$  peak was observed also at around 850 K, and the  $CD_4$  peak was observed at a temperatures by 10–20 K lower than that of graphite. Therefore,  $CD_4$  formation in the CF of 1D-CF/ $B_4C$  is considered to be suppressed due to boron diffusion and solution from the  $B_4C$  matrix into the CF phase in the hot-pressing process.

The effect of boron solution on  $CD_4$  formation in CF is clearly shown in Fig. 7; the relative amount of desorbed  $CD_4$  from graphite was at a higher level than that expected from linear dependence of the amount of desorbed  $CD_4$  on the  $V_f$ , i.e. the surface area density of the CF phase. Also, it is considered that boron solution in the CF does not depend on the  $B_4C$  fraction in the 1D-CF/ $B_4C$  when the

sintering temperature and time condition are the same. The diffusion depth of boron atoms into CF in the 1D-CF/ $B_4C$ 's is principally controlled by the sintering temperature.

The amount of desorbed  $CD_4$  for P65(1700) and that for P65(1800) were both higher than that for P65(2100) as shown in Fig. 7, which is considered to be due to the lower boron concentrations in the CF.

As shown in Fig. 3, the chemical sputtering rate of the CF in 1D-CF/ $B_4C$  sintered at 1700°C is considered to be close to that of pure graphite. In the case of 1800°C, chemical sputtering of the CF phase is suppressed as far as to be judged from Fig. 3. However, as shown in Fig. 5, boron diffusion has not taken place sufficiently to suppress chemical sputtering of the CF's at the core region completely. In the present experimental conditions, it was concluded that the sintering temperature for suppression of chemical sputtering of the CF should be at least higher than 1800°C, and preferably higher than 2100°C, at least for 'high-temperature' erosion region in which boron addition is effective [12].

#### 5. Summary

Erosion and TDS characteristics under 1 keV  $D^+$  irradiation were investigated for 1D-CF/ $B_4C$  of  $V_f$  at 30–80 vol%, hot pressed at 1700–2100°C, cut normal to the CF axis, which was developed as PFM of long life time and high thermal conductivity compared to  $B_4C$ -overlaid graphite. The measured erosion yield of the 1D-CF/ $B_4C$  sintered at 2100°C and 1800°C was found to be lower than the value calculated from those of the constituent  $B_4C$  and graphite phase basing on a simple sum rule. For the case of 1D-CF/ $B_4C$  sintered at 2100°C, a main  $D_2$  peak at 850 K, a shift of the  $CD_4$  peak toward lower temperature, and the suppression of chemical sputtering of the CF at the core region were observed. These were ascribed to the boron diffusion into the CF core. And it was also concluded, that the boron concentration in the CF mainly depends on the sintering temperature and time. In the case of sintering temperature below 1800°C, the boron diffusion was not sufficient to suppress chemical sputtering of the CF's at the core region.

#### References

- [1] T. Yamaki, Y. Gotoh, T. Ando and K. Teruyama, *J. Nucl. Mater.* 220–222 (1995) 771.
- [2] A. Schenk, B. Winter, C. Lutterloh, J. Biener, U.A. Schubert and J. Koppers, *J. Nucl. Mater.* 220–222 (1995) 767.
- [3] Y. Yamauchi, Y. Hirohata, T. Hino, T. Yamashina, T. Ando and M. Akiba, *J. Nucl. Mater.* 220–222 (1995) 851.
- [4] T. Ando, K. Masaki, K. Kodama, T. Arai, S. Tsuji, T. Sugie, H. Kubo, S. Higashijima, N. Hosogane, M. Shimada, J.

- Yagyu, A. Kaminaga, T. Sasajima, Y. Ouchi, T. Koike and M. Shimizu, *J. Nucl. Mater.* 220–222 (1995) 380.
- [5] R. Jimbou, M. Saidoh, K. Nakamura, A. Akiba, S. Suzuki, Y. Gotoh, Y. Suzuki, A. Chiba, T. Yamaki, M. Nakagawa, K. Morita and B. Tsuchiya, *J. Nucl. Mater.*, to be published.
- [6] Y. Gotoh, T. Yamaki, T. Ando, R. Jimbou, N. Ogiwara, M. saidoh and K. Teruyama, *J. Nucl. Mater.* 196–198 (1992).
- [7] J. Roth, *J. Nucl. Mater.* 176–177 (1990) 132.
- [8] T. Yamaki, Y. Gotoh, T. Ando, R. Jimbou, N. Ogiwara and M. Saidoh, *J. Nucl. Mater.* 217 (1994) 154.
- [9] A. Schenk, B. Winter, C. Lutterloh, J. Biener, U.A. Schubert and J. Kuppers, *J. Nucl. Mater.* 220–222 (1995) 767.
- [10] C. Garcia-Rosales, E. Gauthier, J. Roth, R. Schworer and W. Eckstein, *J. Nucl. Mater.* 189 (1992) 1.
- [11] Y. Hirooka, R.W. Conn, R. Gausey, D. Croessmann, R. Doerner, D. Holland, M. Khandagle, T. Matsuda, G. Smolik, T. Sogabe, J. Whitely and K. Wilson, *J. Nucl. Mater.* 176–177 (1990) 473.
- [12] C. Garcia-Rosales and J. Roth, *J. Nucl. Mater.* 196–198 (1992) 573.